Joint Special Interest Group meeting between euspen and ASPE
Dimensional Accuracy and Surface Finish in Additive Manufacturing,
KU Leuven, BE, October 2017
www.euspen.eu

Loss of dimensional accuracy due to non-uniform shrinkage in additively manufactured polymer parts fabricated by two-photon lithography

Vu H. Nguyen, Jefferson A. Cuadra, Chuck Divin, James S. Oakdale, Sourabh K. Saha

Lawrence Livermore National Laboratory, Livermore, CA, USA.

nguyen101@llnl.gov

Abstract

Two-photon lithography (TPL) is a popular technique to additively manufacture complex 3D structures with submicron building blocks. This technique uses a nonlinear photo-absorption process to polymerize submicron features within the interior of a photopolymer resist. As the polymerization process involves a change in the physical state from a liquid photopolymer to a crosslinked solid, polymerization is often accompanied with volumetric shrinkage. To fabricate dimensionally accurate parts in TPL, one must carefully account for this shrinkage. Traditionally, this shrinkage is compensated during part design by modeling it as a uniform volumetric shrinkage. Herein, the assumption of uniform shrinkage being inaccurate in case the fabricated parts contain non-uniform features is validated. The non-uniform features demonstrated in this work are internal cavities. To quantify the non-uniform shrinkage during TPL, 3D structures with internal cavities are fabricated with the cavities fully enclosed by partly porous walls. To visualize the internal features, a custom radiopaque resist for TPL was synthesized so that the local intensity of X-ray image represents the depth-averaged material density. It is observed that linear shrinkage is non-uniform and varies from 0.7% to 6.1% within the same part in the presence of internal cavities. This non-uniformity occurs due to a combination of (i) the large dimensional changes due to the structural deformation of the features and (ii) the increase in the density of the material during curing. The quantitative shrinkage data generated herein can be used to achieve high dimensional accuracy by implementing compensation algorithms when designing TPL parts.

Additive Manufacturing, Two-Photon Lithography, Volumetric Shrinkage, X-ray Computed Tomography

1. Introduction

Two-photon lithography (TPL) has been extensively used in the last two decades to additively manufacture polymer parts with submicron features for applications such as microfluidics [1], mechanical metamaterials [2], and photonics [3]. Although TPL enables printing of complex 3D structures, the dimensional accuracy is limited by the shrinkage of the features during printing. The amount of linear shrinkage in TPL has been previously reported to vary from a few percent [4] to 18% [5] at the top of log piles, up to 14% at the top of cuboid structures [6], and up to 45% for the thickness of suspended single lines [7]. Possible causes of the shrinkage in TPL include (i) the increase in the mass density of the resist during polymerization, (ii) the partial or full collapse of the porous polymer structures formed upon removal of unsolidified resist during development, and (iii) the effect of the capillary forces during drying [7, 8].

Several approaches have been demonstrated in the past to overcome the errors caused by the shrinkage [4, 9–12]. For example, Sun *et al.* designed their structures to pre-compensate the shrinkage in log-pile structures for photonic crystals by empirically quantifying the shrinkage [4]. Lim and co-workers developed a contour offset algorithm where a 2-D outer-contour matrix of an initial design was constructed [9]. The offset was calculated based on the TPL voxel size, the size of the designed 2-D structure, and its pattern. In addition, several groups have focused on developing low-shrinkage TPL resists [10–12].

Despite the critical role of shrinkage on the dimensional accuracy of parts printed via TPL, the variation in volumetric shrinkage within a single heterogeneous structure has not been studied in the past. In this work, the shrinkage in TPL-printed parts with internal cavities bounded by both non-porous and partly porous walls are quantified. Scanning Electron Microscope (SEM) images and X-ray radiographs are used to study the shrinkage. The experimental results in this work reveal that the shrinkage in a partially drained cavity with porous walls is high whereas the shrinkage in a non-drained cavity with solid walls is low.

2. Method

In this study, the commercially available Nanoscribe Photonic Professional GT system is used to implement two-photon lithography. This system utilizes a 100 fs fibre laser with a repetition rate of 80 MHz to locally polymerize a photo-curable resin. A schematic of the process is shown in Fig. 1.

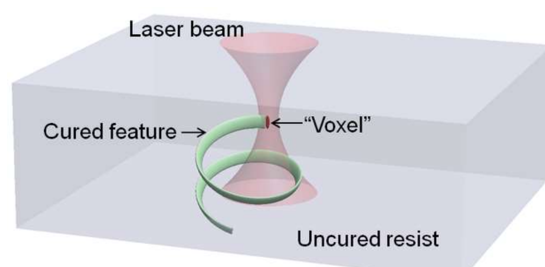

Figure 1. Schematic of two-photon lithography.

During curing, the resin is locally transformed from a liquid state into a solid state. This change in phase is accompanied with an increase in the material density that leads to the shrinkage of the features. Non-uniform shrinkage is observed when the part comprises both solidified and uncured resin in an enclosed cavity. To quantify the shrinkage in the parts with internal cavities, a custom radiopaque acrylate resist that can be imaged via X-rays was synthesized. This radiopaque resist contains 10% to 25% by weight of iodine in the form of an iodized aromatic acrylate pre-polymer, a high-efficiency photoinitiator for two-photon lithography, and acrylate pre-polymers.

To study the shrinkage in TPL parts, two sets of experiments are performed. In the first set of experiments, the shrinkage in solid cylindrical homogeneous structures without internal cavities is quantified. In the second set of experiments, the shrinkage in a cylindrical heterogeneous structure with four internal cavities is quantified. The parts without an internal cavity were printed at a laser power of 20 mW and 25 mW, scanning speed of 10 mm/s, and with a 1 µm vertical spacing between adjacent layers. The printed parts were then coated with 2 nm of gold and imaged on a Phenom Desktop SEM to quantify the shrinkage of the part, as can be seen in Fig. 2 below. Four cylinders grouped and printed close to each other have the same designed in-plane line spacing and laser power.

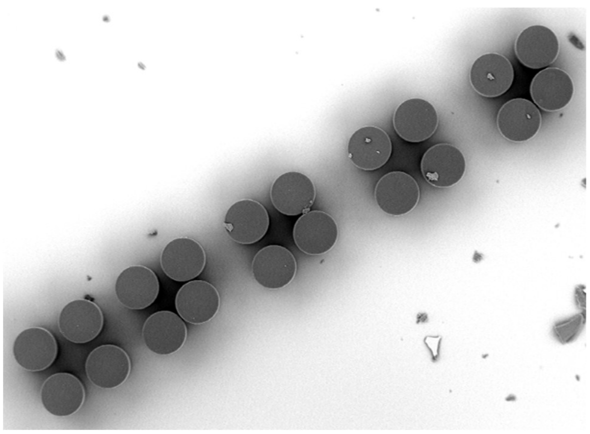

Figure 2. SEM image of the solid cylindrical homogeneous structures without internal cavities.

The cylindrical part with internal cylindrical cavities were printed by the same Photonic Professional GT system and imaged using an X-ray imaging system that has an 8 keV X-ray source (Zeiss UltraXRML200). This system was used to generate radiographs of the cylindrical sample. A part with four cylindrical sections stacked vertically was printed at a writing speed of 20 mm/s and average laser power of 20 mW. Each of these four sections had a designed height of 25 µm, a designed diameter of 55 µm, and contained an internal coaxial cylindrical cavity. During printing, the resist within this designed cavity region is left un-polymerized. After development, this uncured resist either leaks out of the cylinder or stays fully enclosed, depending on the porosity of the cylinder's wall. To study this resist leakage during development, the cylindrical structure was designed so that the wall thickness of the cylindrical sections varies along the cylinder's length. The wall thickness of the annular rings surrounding the four cavities were 10 µm, 5 µm, 5 µm, and 5 µm from bottom to top. In addition, to study the effect of porosity of the walls, the in-plane line spacing of the line features were designed to be 0.4 µm, 0.09 µm, 0.4 µm, and 1 µm (bottom to top). The out-of-plane vertical spacing was held at 0.6 µm throughout the part. As the line width is smaller than 0.5 µm, the part with the line spacing of 1 µm is expected to be fully porous. The discretized model of the heterogeneous part is shown in Fig. 3.

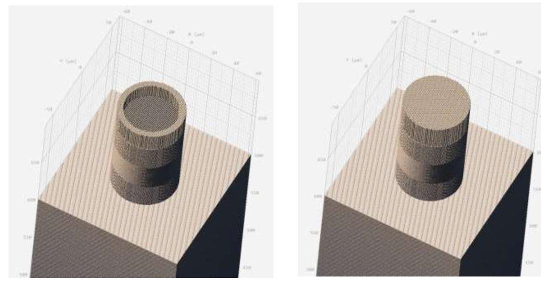

(a) (b)

Figure 3. 3-D rendering of the part with simulated voxel lines showing (a) the top cavity and (b) the completed part. The base has a 125 µm square cross-section.

3. Results and Discussions

3.1 Shrinkage in Homogeneous Parts

The variation in shrinkage in homogeneous solid cylindrical pillars with laser power and in-plane line spacing is shown in Fig. 4. The error bars represent the standard deviation obtained from a sample size of four pillars. It is expected that the shrinkage in the part would increase with an increase in the line spacing due to a decrease in the structural strength of the part. This expectation is supported by the experimental data summarized in Fig. 4. It has been observed that the linear shrinkage in the lateral dimension of a solid part varies between 5% to 6%.

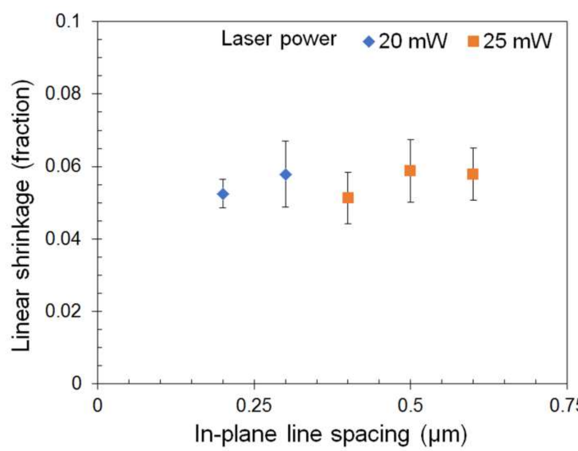

Figure 4. Effect of line spacing and laser power on linear shrinkage.

3.2 Shrinkage in Heterogeneous Parts

A radiograph of the cylindrical part with four cavities is shown in Fig. 5. In this part, the top section has collapsed due to low structural rigidity of the porous top structure that has a line spacing of 1 µm. As a result of the porous structure, the cavity inside this section is fully drained. This can be confirmed from the radiograph wherein the colour intensity (blue to yellow) represents the amount of X-ray absorption. Due to structural collapse, the diameter of the cylinder around this cavity is lowest. The cavity immediately below this has partially porous walls; the wall porosity of the next cavity (3rd from top) is higher than that of the one immediately above it. This is unexpected as the line spacing for the 3rd cavity is lower than that of the cavity that is 2nd from top (0.09 µm vs 0.4 µm). Finally, the bottom-most cavity is fully enclosed suggesting that the thicker wall (10 µm vs. 5 µm) is non-porous. As this section is close to the base, the shrinkage of this section is influenced by the shrinkage of the base. The shrinkage of the four sections is listed in Table 1. The shrinkage in the part is a combination of (i) the change in the density of the part upon curing and (ii) the structural deformation of the part based on the stiffness of the part and the capillary forces encountered during development. The effect of changing the density of the cured features is evident from the lower shrinkage in the 2nd and 3rd cavities relative to the base of the part. In addition, the structural collapse of the part (as observed in the top-most section) leads to deformations that confound the material density based shrinkage.

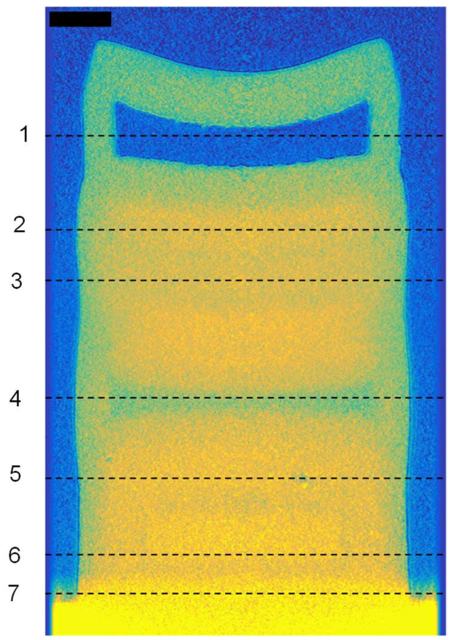

Figure 5. X- ray radiograph of the cylindrical heterogenous part with four internal cavities. The horizontal lines indicate the cross-sections at which the diameters were measured. The scale bar is 10 µm long.

Table 1. Shrinkage at different sections of the heterogenous part.

Cross-section porion	Designed diameter (µm)	Measured diameter (µm)	Linear shrinkage (%)
1	55	51.62	6.14
2	55	54.23	1.40
3	55	53.27	3.14
4	55	54.61	0.71
5	55	53.53	2.67
6	55	53.78	2.22
7	55	54.16	1.53

4. Conclusions

In this work, it is demonstrated that the shrinkage during two-photon lithography is a combination of the increase in the structure's density upon curing and the deformation of the structure under the influence of capillary forces during development. A part with a uniform layout of the elementary line features demonstrates uniform shrinkage for the sections that are sufficiently far away from the base. However, the shrinkage in the structure is non-uniform in the presence of structural heterogeneity. This structural heterogeneity could either be in the form of enclosed cavities filled with uncured liquid resist or slender features that have a low structural rigidity. When dimensional accuracy is critical, one must carefully account for this non-uniform shrinkage.

Acknowledgements

This work was performed under the auspices of the U.S. Department of Energy by Lawrence Livermore National Laboratory under contract DE-AC52-07NA27344. (Document # LLNL-ABS-730141) Funding was available from LDRD project #16-ERD-047.

References

[1] Maruo S, and Inoue H 2006 *Appl. Phys. Lett.* **89**(14) 144101.
[2] Meza L R, Das S, and Greer J. R. 2014 *Science* **345**(6202) 1322-1326.
[3] Von Freymann G, Ledermann A, Thiel M, Staude I, Essig S, Busch K, and Wegener M 2010 *Adv. Func. Mat.* **20**(7) 1038-1052.
[4] Sun H-B, Suwa T, Takada K, Zaccaria P, Kim M-S, Lee K-S, and Kawata S 2004 *Appl. Phys. Lett.* **85** 3708–10.
[5] Ovsianikov A, Shizhou X, Farsari M, Vamvakaki M, Fotakis C, and Chichkov B N 2009 *Opt. Express* **17** 2143–48.
[6] Li Y, Qi F, Yang H, Gong Q, Dong X, and Duan X 2008 *Nanotechnology* **19** 055303.
[7] Takadaa K, Sun H-B, and Kawata S 2006 *Proc. SPIE* **6110** 61100A-1.
[8] Jiang L J, Campbell J H, Lu Y F, Bernat T, and Petta N 2016 *Fusion Sci. and Tech.* **70** 295–309.
[9] Lim T W, Park S H, and Yang D-Y 2005 *Microelect. Eng.* **77** 382–88.
[10] Baldacchini T, LaFratta C N, Farrer R A, Teich M C, Saleh B E A, Naughton M, Fourkas J T 2004 *J. App. Phys*. **95** 6072–76.
[11] Ovsianikov A, Viertl J, Chichkov B, Oubaha M, MacCraith B, Sakellari L, Giakoumaki A, Gray D, Vamvakaki M, Farsari M, and Fotakis C 2008 *ACS NANO* **2** 2257–62.
[12] Yee D W, Schulz M D, Grubbs R H, and Greer J R 2016 *Adv. Mater.* **29** 1605293.